THE INSTITUTE FOR SYSTEMS RESEARCH

ISR TECHNICAL REPORT 2008-22

Particle Steering by Active Control of Magnetic Fields, and Magnetic Particle Agglomeration Avoidance

Lin, John, Advisor: Shapiro, Benjamin, Graduate Student: Probst, Roland

The Institute for Systems Research

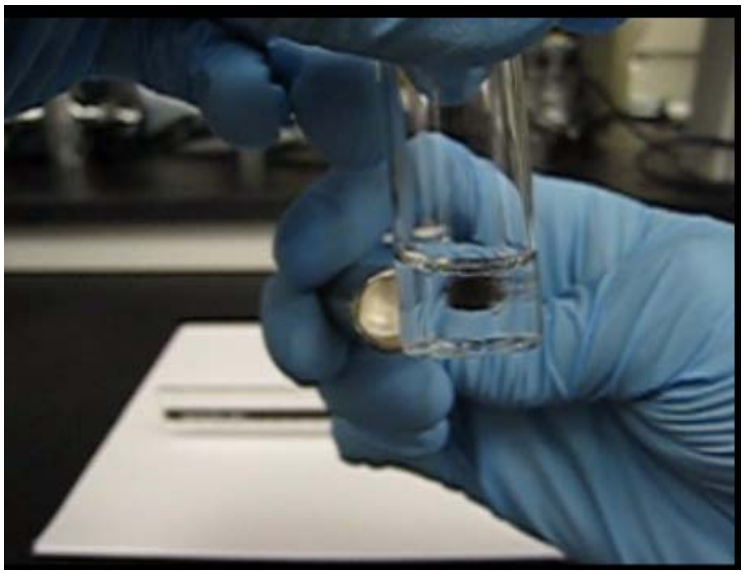

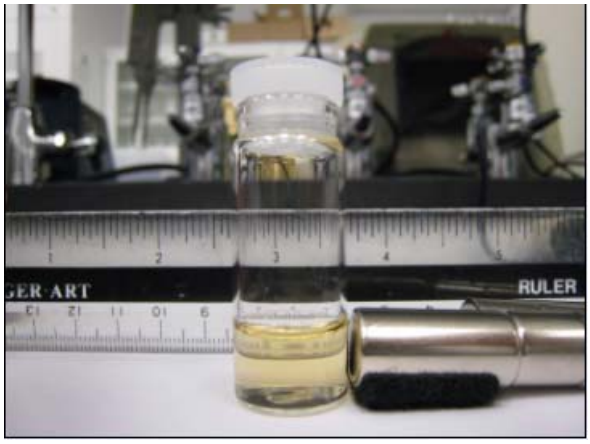

John Lin

Particle steering by active control of magnetic fields, and magnetic particle agglomeration avoidance

A. JAMES CLARK SCHOOL OF ENGINEERING

RESEARCH PAPER

Particle steering by active control of magnetic fields, and magnetic particle agglomeration avoidance

John Lin [c], Benjamin Shapiro [a], Roland Probst [b]

[a] Associate professor at the University of Maryland, in the Aerospace engineering dept
[b] Graduate student with Shapiro
[c] Undergraduate student with Shapiro, in the Institute of Systems Research department

Abstract

Concerns dealing with the application of superparamagnetic ferrofluid as a drug carrier are studied both experimentally and theoretically. A dynamically controlled electromagnet experiment was designed to focus a stable ferrofluid trap at a specified distance. A theoretical magnetic driving force equation has been compared to experimental results for verification; verification was not achieved. Particle chaining avoidance theory is discussed based on previous research done by other sources.

1. Introduction

For the last thirty years, ferrofluids with superparamagnetic properties have had significant interest in the biomedical field [1]. These ferrofluids exhibit characteristics similar to paramagnetic materials except that their magnetization in low to moderate fields is much larger. Due to these characteristics, research is being done on the use of these ferrofluids as a method to carry drugs to targeted locations within the human body using external magnets as the driving force. However, there are several major problems that arise when attempting to use this method of drug delivery; only a few will be discussed here. The first problem is the ability to create a stable ferrofluid trap at a certain distance from a magnet. Earnshaw's theorem states that there cannot be a stable trap formed using superparamagnetic particles within a permanent magnetic field. Another problem is characterizing the driving force on the ferrofluid blob. This driving force is necessary for the ferrofluid blob to maintain stability while moving, and to overcome other forces

experienced when traveling through the vascular system; such as blood flow. The last problem to be discussed is particle chaining. Ferrofluids within a sufficient magnetic field can form particle-particle chain like agglomerates which can cause a severe health hazard to patients.

The objective of this work is to discuss and provide solutions to these problems. To overcome Earnshaw's equation, an experiment using alternating electromagnetic fields was designed to create a stable ferrofluid trap at a specific distance. To address the issue of characterizing the necessary driving force for ferrofluid control, a theoretical driving force equation was compared with experimental results for verification; verification was not achieved. Finally, a particle chaining avoidance theory was developed using previous experimentation from other research.

2. Stable Ferrofluid Trap

Permanent magnetic fields can only focus ferrofluid particles near the surface of the skin; magnets of maximum FDA regulated strength can only create a less than 5cm deep focus [2]. This is a fundamental consequence of the classic Samuel Earnshaw 1842 theorem [3], and is one of the major limitations for the clinical use of this drug focusing method. However, in theory, Earnshaw's limitation for permanent magnets can be bypassed if the magnetic fields vary in time [2]. Therefore, to test this theory, we have designed an experiment using dynamically controlled electromagnets to create an alternating magnetic field for deep surface particle stabilization and control. The experiment should be ready for testing in two weeks. Currently, we have designed two electro magnet arrangements for experimentation. The first arrangement is shown to the right in figure 1.

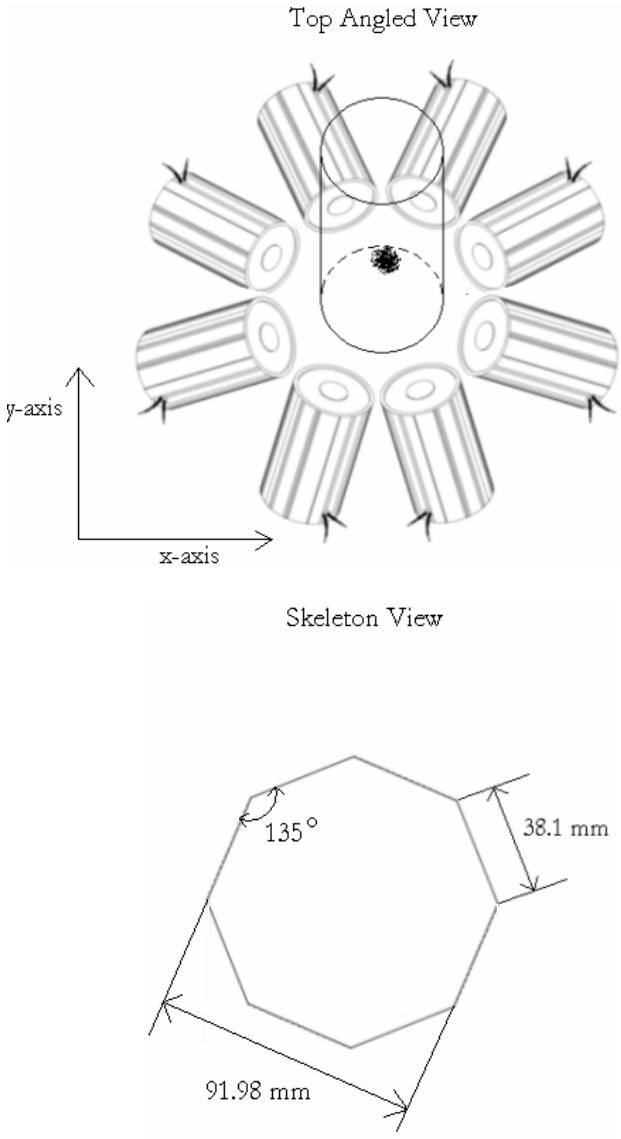

Fig. 1. Eight electromagnets surround a glass vial containing the ferrofluid Magnetite (Fe3O4), indicated by the black dots, in a DI H2O environment with a glycerin bottom layer. Filled view is shown on top and skeleton view on bottom.

The second arrangement is shown below in figure 2.

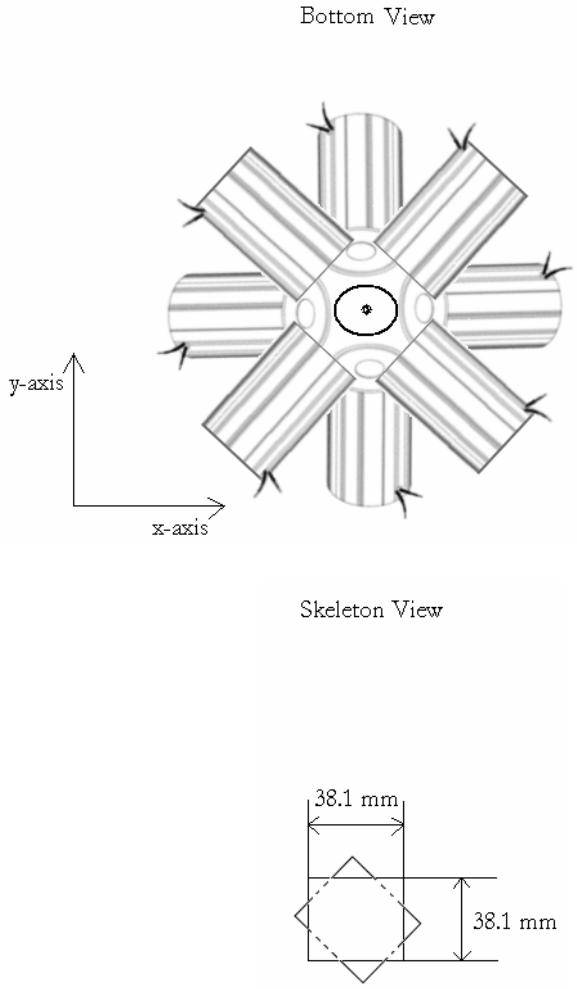

Fig. 2. Four electromagnets placed in a square configuration in the x-y plane, and four electromagnets placed diagonally oriented down surround a glass vial containing the ferrofluid Magnetite (Fe3O4), indicated by the black dots, in a DI H2O environment with a glycerin bottom layer. Filled view is shown on top and skeleton view on bottom.

Arrangement 1 was designed to provide precise ferrofluid blob maneuvering within two dimensions. However, due to the arrangement, there is a limitation on how close the electromagnets can be to the ferrofluid; this creates a limitation on magnetic driving force, which limits particle control. Arrangement 2 was designed to have three dimensional control; using gravity as the negative z-axis driving force. Because there are less electromagnets per plane as compared to arrangement 1, there is a limitation on precision of particle movement. However, the electromagnets' maximum distance from the ferrofluid is 38.1 mm as compared to 91.98 mm in arrangement 1; allowing for stronger applied magnetic driving forces, which increases particle control.

2.1 Materials

Materials include electromagnets, USB DAQ module, custom power supply, 1μm ferrofluid particles, glycerin, DI water, glass vial, and adjustable mounts for arrangement 2. The purpose of and where to obtain each material will now be discussed.

The electromagnets were chosen for their relatively large magnetic force B created off the electromagnet surface, and because the power source could be conveniently customized to our needs. The above distances shown in the skeleton view of each arrangement is calculated for the electromagnet dimensions given below.

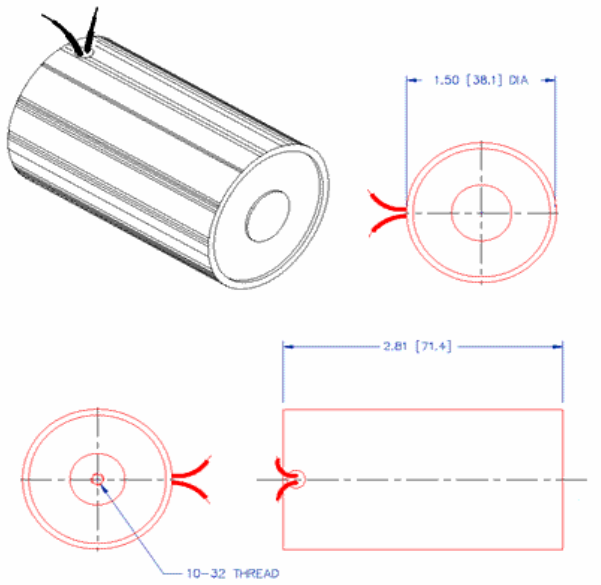

*Note that the electromagnets can be kept on for 180 seconds before over heating; let cool for 3 times as long as was on.

Only the circular core of the electromagnet produces the magnetic field so the fear of magnet-magnet collision due to the close placement of neighboring electromagnets is not a limiting factor. The electromagnet's vender is solenoidcity and can be ordered from (http://www.electromechanicsonline.com/product.asp?pid=559).

The USB data acquisition (DAQ) module allows a computer to dynamically control the turning on and off of electromagnets, and electromagnet strength for precise particle movement; Lab view software is used as the computer user interface. A picture of the DAQ module is shown below.

The DAQ module's vender is Measurement Computing (http://www.measurementcomputing.com/index.html).

A custom power supply is necessary because the DAQ module can only output +- 10 volts and 3.5 mA; not enough to power 8 electromagnets. Therefore a power supply with a linear power increase and accurate voltage and ampere outputs will be used. The power supply vender is Acopian power system builder (http://www.acopian.com/powersys.aspx).

*Power source substitute: For a cheap portable power source, the electromagnets should be able to run on common supplies found in radio shack; see appendix I for wiring schematic. Note that when using this method the power output is not accurate and will only supply power for a few three minute test runs.

1µm ferrofluid magnetite (Fe3O4) particles were used as the particles to be tested on. Particles were chosen for their high magnetic susceptibility. The vender is MagSense (http://magsenselifesci.com/content/view/12/26/).

Glycerin was coated along the bottom of the glass vial indicated in the arrangement figures above, figures 1 and 2, in order to reduce particle to glass friction along the bottom surface of the vial. The ferrofluid particles are somewhat non-poplar so they tend to float along the surface of the glycerin, allowing for easier particle movement. A picture of described particle floating is shown below in figure 3.

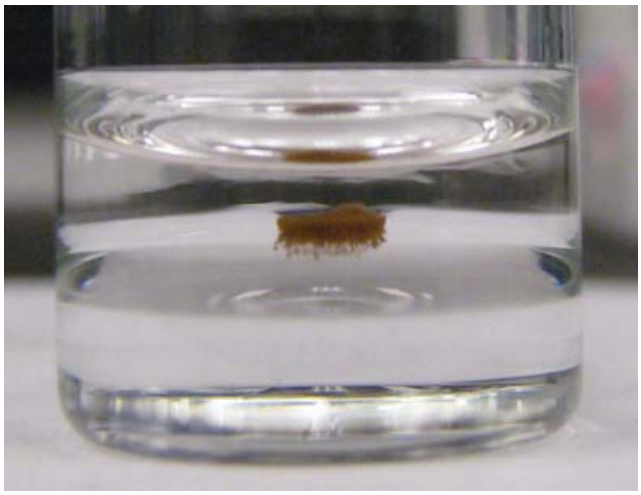

Fig. 3. Ferrofluid Magnetite (Fe3O4) is shown floating on top of glycerin in DI water layer with no external magnetic field applied.

The vender for the glycerin is Fisher Chemicals (http://www.fishersci.com/wps/portal/HOME).

DI water was used as a low viscous environment for the ferrofluid particles to travel in, and to show that stability and control could be achieved in an aqueous environment.

A general glass vial was used to hold the glycerin – water bilayer with ferrofluid particles. The glass will have no effect on the magnetic field experienced by the ferrofluid.

Adjustable 6 inch high Panavise 846-06W Micro CCTV camera mounts were used to diagonally direct the electromagnets seen in arrangement 2. The camera mount is shown below.

The vender is Buy.com

3. Driving force characterization

The external magnetic field produces the driving force necessary for particle control. This driving force may need to increase or decrease according to the human vascular environment that the particles are in; for example, to overcome different blood flow rates. This creates a need to characterize the magnetic driving force in order to more precisely control the particles.
The force density (units N/m^3) on a fluid element of a ferrofluid is [4]

$$\vec{f}_{mag} = \frac{2\pi a^3}{3}\mu_0 C \frac{\chi}{1+\chi/3}\nabla\left(\vec{H}^2\right) \quad (1)$$

where a [m] is the particles radius, μ0 = 4 π × 10−7 [V s / A m] is the permittivity of vacuum, C is the concentration [particles number per m^3], χ is the magnetic susceptibility [non-dimensional], and H in SI units [A/m] is the externally applied magnetic field intensity. We have developed an experiment using an electromagnet as the Fmag source to verify that this representation of magnetic driving force applies to our application.

3.1 Theory behind verification experiment

If we apply an external magnetic driving force on the ferrofluid, while the ferrofluid is immersed in an aqueous environment with similar polarity to negate surface tension of the ferrofluid blob, then the only two forces acting on the particle in the x-y plane would be force due to magnetization (Fmag), and force due to drag (Fdrag). Both of these forces can be seen to be dependent on distance between electromagnet and ferrofluid on time, x(t). Summing these two forces will provide a net force (Fnet). This Fnet can be divided by mass to obtain acceleration from Newton's second law, and because acceleration is a second order differential equation, the theoretical time necessary for the ferrofluid to travel a certain distance can be obtained. This theoretical time can then be compared to experimental time taken over a same chosen distance. Similar time results between theory and experimental would indicate that the Fmag equation provided in equation (1) is suitable to represent the magnetic diving force applied to the ferrofluid particles. Equations and calculations for this theory are now described.

3.2 Verification experiment calculations

It is first necessary to show that the magnetic flux B produced by an electromagnet is dependent on distance between electromagnet surface to ferrofluid particles on time, x(t). Using Biot-Savart law written for currents, the magnetic flux B produced at a certain distance by a general current loop found in an electromagnet can be represented as [5]

$$\vec{B}_{loop} = \frac{\mu_0}{2\pi}\frac{I R^2}{\left(x(t)^2 + R^2\right)^{3/2}} \quad (2)$$

where I is the current in [A], R is the radius of the coil within the electromagnet [m], $\mu 0 = 4\pi \times 10{-}7$ [V s / A m] is the permittivity of vacuum, and x(t) is the time dependent distance between the surface of the electromagnet and the ferrofluid particles. Gathering constants together and factoring in the number of current loops within the electromagnet, the Bloop equation can be used to approximate a B equation for electromagnets;

$$\vec{B}_{Emag} = \frac{K}{(x(t)^2 + R^2)^{3/2}} \quad (3)$$

where K is a constant. K can then be adjusted so that the theoretical B_{Emag} matches experimental B_{Emag} values.

In this experiment, a tubular electromagnet from solenoid city (http://www.electromechanicsonline.com/product.asp?pid=524) was used to test the theoretical B_{Emag} equation. Results are shown below in figure 4.

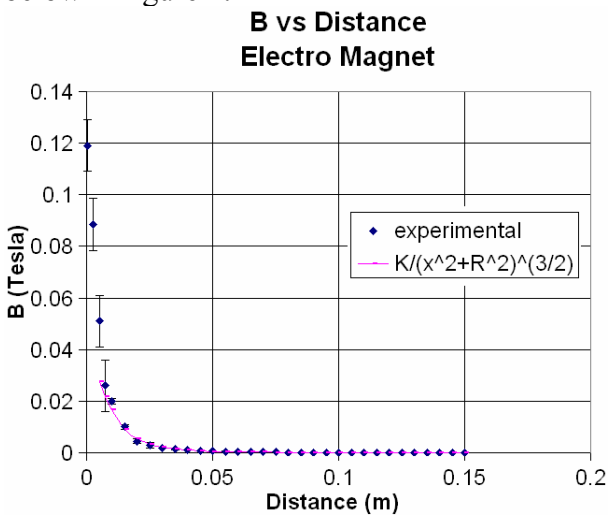

Fig. 4. Theoretical magnetic flux values are compared to experimental values over distance. Theoretical values are within experimental error bars. Experimental values are measured with a Bell 640 incremental F.W. Gauss meter with a T-640-462 probe.

The results show that experimental data from 1cm to 4 cm has on average a less than 15% error with theoretical values, and is within the error bars. Because this data lies within the experimental error, B_{Emag} theory is accurate enough to represent the magnetic flux produced off the surface of an electromagnet. B_{Emag} from 1cm to 4cm can now be used in the following equations explaining the theory in section 3.1.

We will now go into the calculations behind the theory in section 3.1.

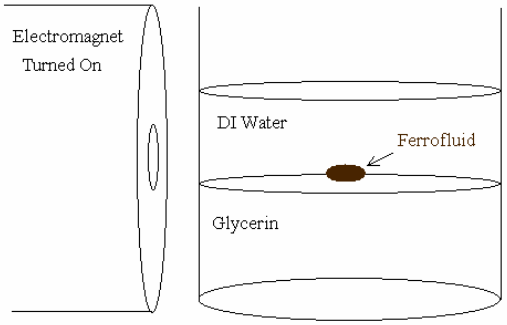

Force Diagram

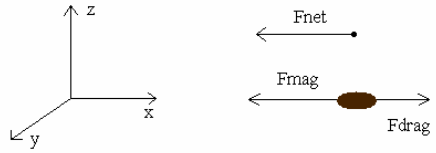

Summing forces on the ferrofluid blob in the x-y plan gives

$$Fmag - Fdrag = Fnet \quad (4)$$

Using Fmag provided in equation (1) and the Stokes drag on a spherical particle in a liquid [6] as Fdrag, equation (4) becomes

$$\frac{2\pi a^3}{3}\mu_0 C \frac{\chi}{1+\chi/3}\nabla\left(\vec{H}^2\right) - 6\pi a\eta\vec{V}_r = Fnet \quad (5)$$

where η is viscosity [N s/m^2], and V_r is relative velocity [m/s].

Provided that the relationship between B and H when a generated magnetic field passes through a magnetic material is [4]

$$B = \mu_0(H+M) \tag{6}$$

, and

$$M = \chi H \tag{7}$$

due to weak field approximation [7], then equation (6) can be arranged in the form of

$$\vec{H} = \frac{\vec{B}_{mag}}{\mu_0 (1+\chi)} \tag{8}$$

Substituting B_{Emag} from equation (3) and H from equation (8) into the force equation (5) then dividing by mass to get ferrofluid acceleration, equation (5) becomes

$$\frac{\frac{2\pi a^3}{3\mu_0} C \frac{\chi}{1+\chi/3} (K^2) \left(\frac{1}{x(t)}\right) \left(\frac{1}{(x(t)^2+R^2)^3}\right) - 6\pi a \eta \dot{x}(t)}{\text{Mass}} = \text{FerroFluid acceleration} \tag{9}$$

With equation (9), it is now possible to verify the force equation (1)'s accuracy.

3.3 Results

The ferrofluid acceleration function was solved numerically as a second order differential equation using the software MatLab's ODE45 function. This produced a model of the distance the ferrofluid blob traveled versus time. This theoretical time was compared to experimental times taken over the same distance of 2.5 cm to 1.0cm (the distance between one end of the glass vial to the other); similarity between the times would indicate that Fmag is a reasonable representation of the driving magnetic force on the ferrofluid blob. No verifiable results were obtained. The theoretical values exceeded the experimental error of observed times. The high errors in the theoretical values are attributed to the FerroFluid acceleration, equation (9). Equation (9) assumes that the ferrofluid travels in a relatively ball shape. However, through observations, the ferrofluid blob has a tendency to travel in a stream like manner. Because of this, equation (9) would have to account for the change in shape from the original ball like ferrofluid blob, and the drag force would need to be represented by another means.

Currently we are designing another verification experiment using a high powered microscope to view the individual 1μm particles. The individual particles should maintain their spherical shape, so the same theory described in section 3.1 and 3.2 will be applied at this micro scale. This should produce very accurate and verifiable results.

4. Particle Chaining Avoidance Theory

Ferrofluids have a tendency to agglomerate at high enough magnetic fields. This can cause blood clots along with other health hazards when traveling through the human vascular system. In order to prevent this agglomeration while maintaining a relatively high magnetic driving force on the ferrofluid for control, particle size, shear rate, magnetic field frequency, and particle surface coating must be considered. The following information is a compilation of particle chaining avoidance data gathered by creditable sources.

4.1 Particle Size

The assumed magnetic driving force per volume on a ferrofluid composed of spherical nano particles is.

$$\vec{f}_{mag} = \frac{2\pi a^3}{3} \mu_0 C \frac{\chi}{1+\chi/3} \nabla\left(\vec{H}^2\right) \tag{1}$$

Equation details found in section 3

One method of increasing this force would be to increase particle size; however as particle

size increase so does the tendency for the particles to agglomerate.

Rosensweig provides particle size limitations to avoid particle agglomeration. His theory is based on a coupling coefficient defined as λ which depends directly on the particle's spherical volume. Therefore, as particle diameter increases, λ increases. Rosensweig tested this theory on a 10 nm and a 13nm diameter particle with magnetization of 446 [kA/m] at a temperature of 298 [K] with coupling coefficients of 1.3 and 2.69 respectively as seen below in figure 5.

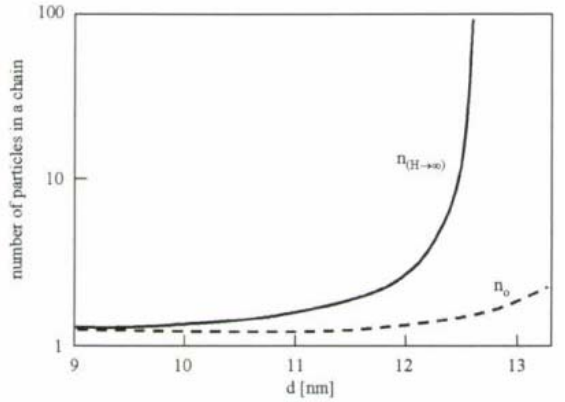

Fig. 5. The length of particle chains in a ferrofluid containing 5 Vol.% of magnetite particles as a function of the particle diameter for vanishing field and for saturation calculated from Rosensweig theory (figure taken from Odenbach [8])

The results showed that the 10nm diameter particle created an average chain length of 1.36 particles, and the 13nm diameter particle created an infinitely long chain length [9]. However, if the magnetization value were to decrease, it would allow for larger particles while maintaining low amounts of chaining. The sacrifice of decreasing magnetization is seen to be advantageous due to Fmag's third power dependence on particle size compared to its first power dependence on magnetization. For example, the particles created by MagSense Corporation have the magnetization characteristics seen in figure 6,

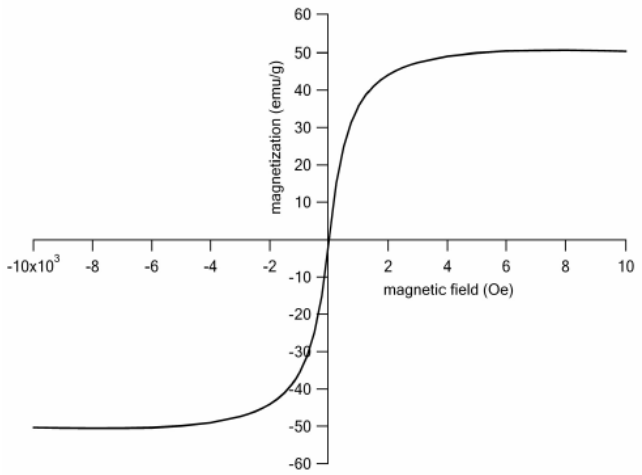

Fig. 6. Magnetization vs. magnetic field intensity characterization of MagSense 1μm particles taken from technical brochure [10].

with a magnetic saturation of 125 [kA/m]. Replacing the 446 [kA/m] magnetization value with 125 [kA/m] in Rosensweig's simulation shows that particle size can increase from 10 nm to 20 nm with chaining; however this low strength chaining can be overcome by the method of shear thinning discussed under the Shear Rate section. This increase in size can more than double the force produced on the magnetic particles.

4.2 Shear Rate

It has been shown that when shear rate increases, the magnetically induced increase of viscosity reduces significantly; this process is known as shear thinning [11]. Odenbach theorizes that as viscosity naturally increases within a magnetic field due to particle agglomeration, shear rate is inducing ruptures in the chain like agglomerates.
After defining forces acting on the chain like agglomerates, and approximating shear rate, it was found that the number of particles in one chain, n_{max} , can be written as

$$n_{max} = \sqrt{\frac{\mu_o}{18\,\eta_o\,\dot{\gamma}}}\; M_o\; \frac{d^3}{(d+2s)^3}$$

Equation details can be found in Odenbach [11]

Because the shear rate, $\dot{\gamma}$, is within a square root, it is seen that increases in shear rate will have a significant effect in lowing number of particles in a chain. Odenbach simulates this equation with a 16nm diameter particle, as seen in figure 7.

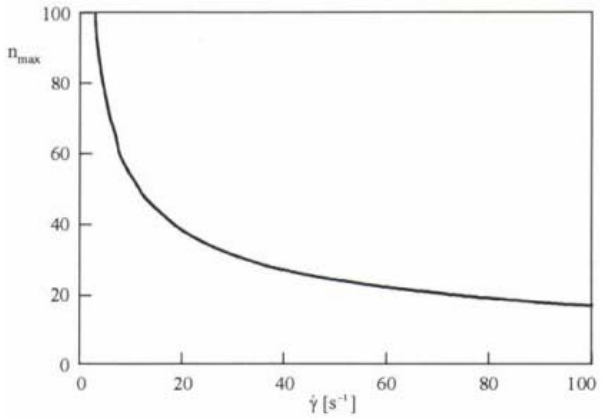

Fig. 7. The dependence of the maximum length of stable magnetic particle chains on shear rate for a particle size of 16nm within a field strength of H=20 [KA/M] (figure taken from Odenbach [12])

The results show a dramatic decrease in particle chaining at well below shear rate levels found near the walls of human blood vessels; which on average is 210 s^{-1}[13]. The data from the simulation shows that particle chain length roughly decreases 70 percent and viscosity decreases over 50 percent due to shear thinning. This indicates that the significant effect of shear thinning can overcome low strength particle chaining near the walls of the blood vessel. For example, it can be seen in figure 8 that shear rates tend to increase near the walls of the artery due to increase flow rates indicated by the dashed lines. On average the shear rate near the wall of this artery is 210 s^{-1}[13]. Therefore, according to Odenbach's theory of shear thinning, a ferrofluid flowing through an artery experiencing particle agglomeration due to sufficient magnetic field intensity will have particle chain lengths larger at regions of low shear rate, near the center of the artery, and smaller at regions at high shear rates, near the wall of the artery. This natural shear rate gradient focuses the ferrofluid in the center of the artery making low strength particle chaining incapable of causing blood flow blockage.

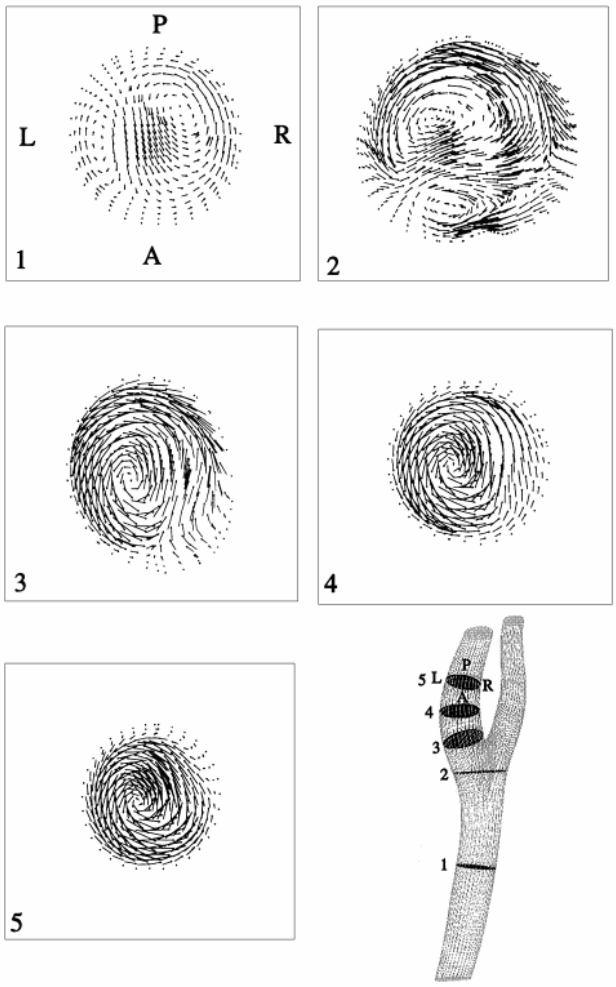

Fig. 8. Anatomically realistic human artery model of secondary pulsatile flow. Artery was simulated numerically [14].

4.3 Magnetic Field Frequency

A phenomenon called negative viscosity occurs in ferrofluids when placed in an alternating magnetic field. If the alternating field frequency is higher than that of the particle's natural rotation, the particles will begin to repel each other creating a negative viscosity compared to its zero external field viscosity [15]. Odenbach tested 10nm Co-ferrite particles within an alternating field ranging from 0 to 1kHz and found that viscosity would significantly decrease as seen in figure 9.

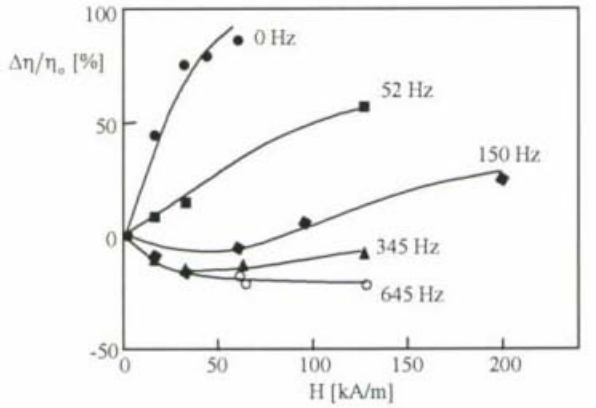

Figure 9. The dependence of the relative viscosity changes of a ferrofluid in an alternating field (after Bacri et al., 1995) (figure taken from Odenbach [16]).

These results indicate that particle agglomeration can be broken up by alternating magnetic fields; however it comes with the cost of losing stable control over the ferrofluid blob due to the particle-particle repelling.

4.4 Particle surface coating

Commercially bought ferrofluid usually have surfactant molecules coated around each particle to avoid particle coagulation. The surfactant molecules act as a method to increase steric repulsion due to steric hindrance as seen in figure 10.

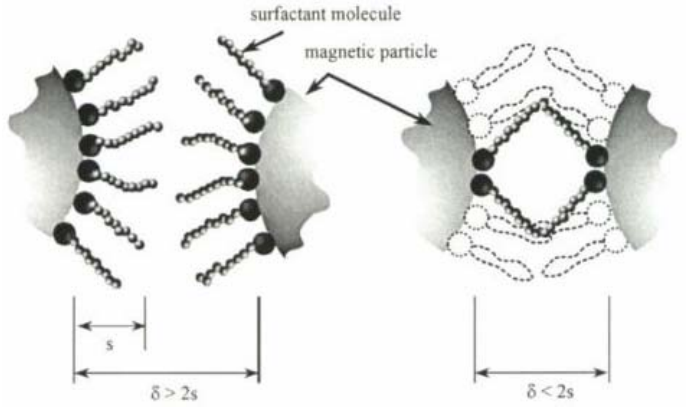

Fig. 10. Surfactant molecules are sterically hindering particle agglomeration (figure taken from Odenbach [17].

Odenbach provides an energy description of the surfactant's contribution to particle-particle repulsion. It can be interpreted from his energy model that although generally manufactured surfactant coatings provide little overall particle repulsion, a little more than what is necessary to overcome Van Der Waals forces, a custom designed surfactant coating would still help the ferrofluid to avoid particle agglomeration.

5. Conclusion

Two machines to produce dynamically controlled alternating magnetic fields with the purpose of producing a stable ferrofluid trap at a certain distance have been designed. Production of these machines should take less than two weeks. The theoretical magnetic driving force on the ferrofluid particles was tested with no verifiable results. The same theory used for testing will be applied at a micro scale level to obtain significantly higher accuracy and verifiable results. Particle chaining avoidance theory was discussed with a focus on the effects of particle size, shear rate, magnetic field frequency, and particle surface coating. Avoidance theory suggests that with manipulation, ferrofluid particles will not cause harmful agglomeration when traveling through the human vascular system.

Appendix I

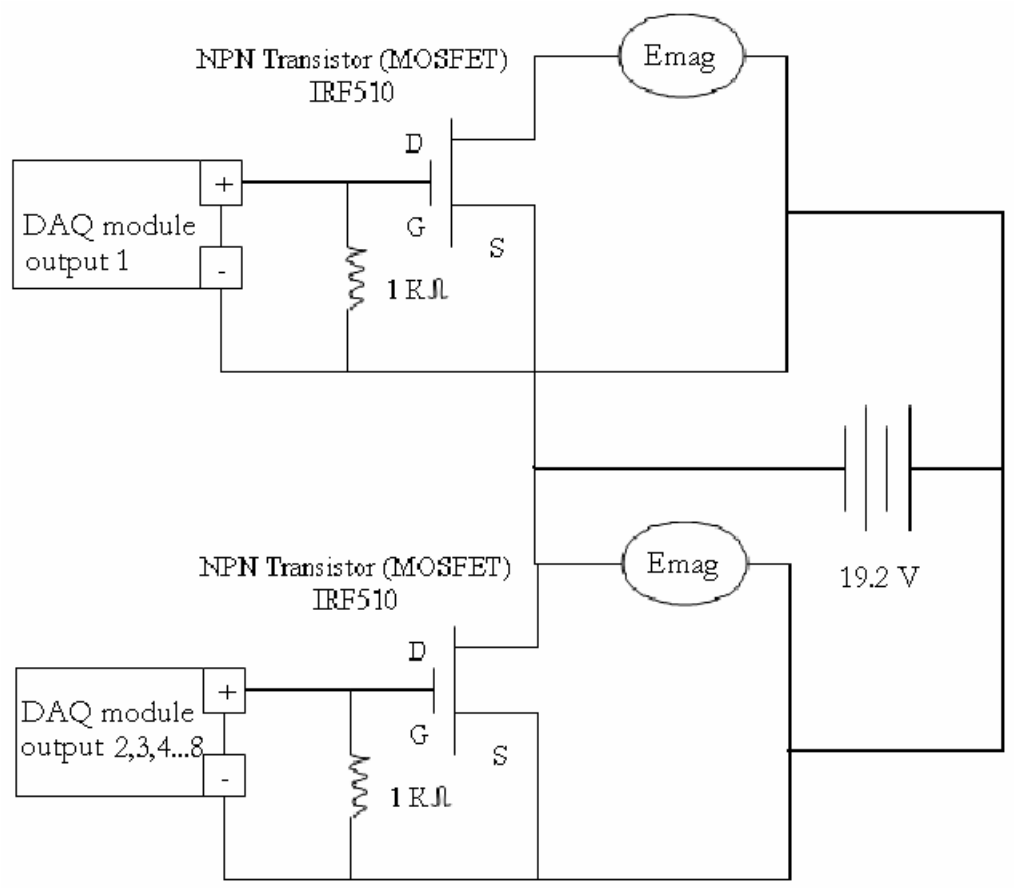

Materials:
+ 8 NPN Transistor (MOSFET) IR510
+ 8 1 KΩ Resistors
+ 2 9.6 volt 1600MAh battery packs
+ Tools for connecting parts together: wiring, solder, etc.

REFERENCES

[1] Lubbe, A.S., Clinical experiences with magnetic drug targeting: a phase I study with 4'-epidoxorubicin in 14 patients with advanced solid tumors. 1996. 56(20): p. 4686-4693.

[2] B. Shapiro, R. Probst, H.E. Potts, D.A. Diver, and A.S. Lubbe, Control to Concentrate Drug-Coated Magnetic Particles to Deep-Tissue Tumors for Targeted Cancer Chemotherapy. 2007. p. 1.

[3] S. Earnshaw, "On the nature of the molecular forces which regulate the constitution of the luminiferous ether," Trans. Camb. Phil. Soc., vol. 7, pp. 97-112, 1842.

[4] R. E. Rosensweig, Ferrohydrodynamics. Mineola, NY: Dover Publications, Inc., 1985.

[5] R.D. Knight, Physics for Scientists and Engineers. San Francisco, CA: Pearson Education, Inc., vol. 4, pp.1004-1008, 2004.

[6] R. F. Probstein, Physicochemical Hydrodynamics: An Introduction, 2 ed. New York: John Wiley and Sons, Inc, 1994.

[7] Odenbach, S. (2002). Magnetoviscous Effects in Ferrofluids. Berlin: Springer. p.53.

[8] Odenbach, S. (2002). Magnetoviscous Effects in Ferrofluids. Berlin: Springer. p.81. Fig. 4.16.

[9] Rosensweig, R.E. (1997). Ferrohydrodynamics. New York: Dover. p.68.

[10] MagSense Life Sciences, Inc. (2008). Technical Brochure.pdf. Retreived July 25, 2008, from Web site: http://magsenselifesci.com/images/pdfs/magsense2.pdf

[11] Odenbach, S. (2002). Magnetoviscous Effects in Ferrofluids. Berlin: Springer. p.78-84.

[12] Odenbach, S. (2002). Magnetoviscous Effects in Ferrofluids. Berlin: Springer. p.84. Fig. 4.18.

[13] Hoeks, A.P.G., et al., Noninvasive Determination of Shear-Rate Distribution Across the Arterial Lumen. 1995. 26(1): p. 26-33.

[14] Zhao, S.Z., et al., Blood flow and vessel mechanics in a physiologically realistic model of a human carotid arterial bifurcation. 2000. 33(8): p. 975-984.

[15] Odenbach, S. (2002). Magnetoviscous Effects in Ferrofluids. Berlin: Springer. p. 52-57.

[16] Odenbach, S. (2002). Magnetoviscous Effects in Ferrofluids. Berlin: Springer. p.55. Fig. 3.14.

[17] Odenbach, S. (2002). Magnetoviscous Effects in Ferrofluids. Berlin: Springer. p.11. Fig. 2.3.